

Role of highly central residues of P-loop and its flanking region in preserving the archetypal conformation of Walker A motif of diverse P-loop NTPases

Ekta Pathak¹, Neelam Atri² & Rajeev Mishra^{1*}

¹Department of Bioinformatics (MMV), Banaras Hindu University, India; ²Department of Botany (MMV), Banaras Hindu University, Varanasi - 221005, India; Rajeev Mishra – Email: mishrarajeev@gmail.com; Phone +91 9935338891; *Corresponding author

Received December 03, 2012; Accepted December 05, 2012; Published January 09, 2013

Abstract:

P-loop NTPases represent a large and highly diverse protein family that is involved in variety of cellular functions. Walker A motif forms a typical arched conformation, necessary to accommodate the phosphate moiety of the nucleoside tri (or di-) phosphate in P-loop NTPases. The feature that maintains the ancient architecture of P-loop is unidentified and uncharacterized. Here, using a well established global network parameter, closeness centrality, we identify that Walker A and its flanking regions (N- and C-terminal) have high density of globally connected residue positions. We find that closeness centrality of these residue positions are conserved across common structural core of diverse domains of P-loop NTPase fold. Our results suggest the potential role of globally connected residues in maintaining the local conformation of P-loop.

Background:

P-loop NTPases represent a large protein family that are involved in variety of cellular functions, for example, in signal transduction, translation, protein transport and localization, signal-sequence recognition, chromosome partitioning, and membrane transport [1-3]. Walker A also known as phosphate binding loop (P-loop) is a common feature of P-loop NTPase fold that bind nucleotide. The consensus sequence of Walker A (GXXXXGK[S/T], where X is any residue) is often used as a motif for identifying new members of this group [4-6]. Walker A sequences are also present in many proteins that do not form P-loop, for example, peroxidases, and enzymes like α -amylase, glutamate dehydrogenase, Taq polymerase, carbonic anhydrase, binding proteins (lectin, trypsin inhibitor), proteases, and others [7]. Here, we investigated the features that maintain the P-loop architecture by employing a well established global network parameter closeness centrality. Protein structures can be represented as a residue-residue interaction network where the residues are nodes and

interactions between them constitute edges. This approach has been useful in various studies like predicting functional residues in enzyme families [8], protein structure flexibility [9], protein folding [10], and side-chain clusters [11]. Closeness centrality is a global network parameter that correlates more accurately with critical residues than any other centrality measurement tested [12]. High closeness residues interact directly or by a few intermediates with all other residues of the protein [13]. By definition, closeness-centrality is calculated by mean distance of a node (residue) to all other nodes (residue) in the network. Amitai *et al.*, [8] have shown that important residue positions like those involved in substrate and co-factor binding, catalysis, and mutation intolerant residues show high closeness centrality in networks. Del sol *et al.* [13] have shown that centrality residues integrate and propagate the information to all other residues in protein.

Here, we show that Walker A and its flanking regions (N- and C-terminal) have high density of high closeness centrality

residue positions in P-loop NTPases. We report that closeness centrality of these residue positions are conserved across common structural core of Ras superfamily and diverse domains of P-loop NTPase fold. No such high densities of high centrality residue positions are observed in the proteins

containing Walker A sequence that do not form P-loop. The presented data clearly indicate the role of globally connected residues in conservation of the local conformation of an ancient motif such as Walker A.

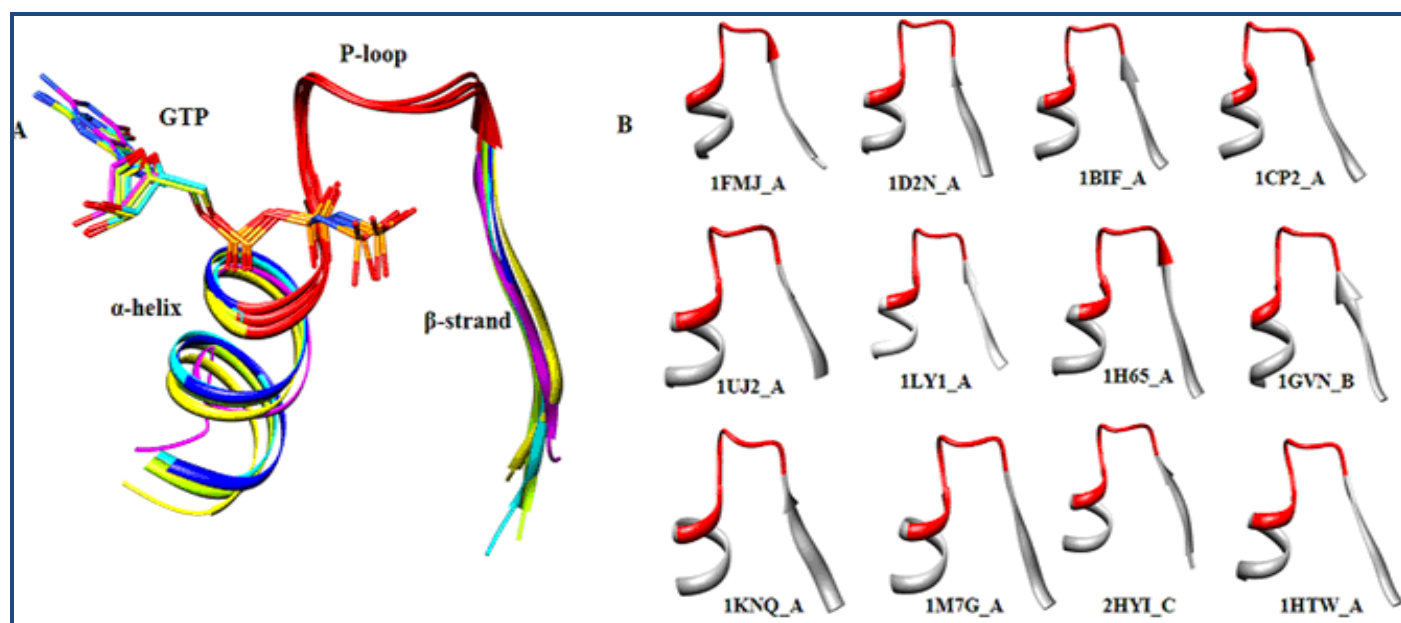


Figure 1: **A)** Ribbon diagram of typical architecture of P-loop (Red) with bound nucleotide molecule (stick) of Ras superfamily proteins [Ras (green), Rab (cyan), Rho (blue), Ran (yellow), and Arf (magenta)]; **B)** Ribbon diagrams of typical architecture of P-loop (red) in representatives of diverse P-loop containing NTPases. 4 letter words are the PDBID.

Methodology:

Selection of structures of P-loop containing NTPases

High resolution X-ray crystallographic structures of diverse domain of P-loop containing NTPases were used in the study. Initially, ScopTree search of protein databank (<http://www.rcsb.org/pdb>) was used to retrieve a set of 1203 structures of P-loop containing nucleoside triphosphate hydrolase. The search was then refined to 227 distantly related protein structures by using ScopTree homologue removal tool at 30% sequence identity cutoff. This was primarily done to avoid redundancy and utilize the diversity present in the P loop NTPases. Complete structures (i.e., without chain breaks or missing residues) with resolution ≤ 2.4 were chosen. Finally, we selected 23 structures of P-loop NTPases **Table 1** (see **supplementary material**). We retrieved 22 PDB files for protein structures containing Walker A sequence (GXXXXGKS/T) that do not form the P-loop **Table2** (see **supplementary material**) [7].

Computation of closeness centrality

Protein structures can be represented as a residue-residue interaction graphs in which amino acid residues serve as the nodes and their interatomic contacts are the edges. Closeness centrality correlates more accurately with critical residues than any other centrality measurement tested [12]. Therefore, we used SARIG server which efficiently calculates the closeness centrality (please see **supplementary material for calculation and explanation**).

Beginning with the atomic coordinates of a protein structure, server calculates the interaction between each pair of atoms by using the CSU program [14]. Closeness values were calculated

for each residue and standardized by calculating their standard deviation from the mean value. The z-score of the closeness centrality was calculated by $z\text{-score} = (C(x) - \mu) / \sigma$, where μ is the mean value of closeness and σ is the standard deviation. The residues with $z\text{-score} \geq 1.0$ were considered significant (for detailed descriptions, please refer to Amitai *et al* [8]). Protein structure analysis was performed using Chimera (<http://plato.cgl.ucsf.edu/chimera>).

Results and Discussion:

Walker A motif forms a typical architecture in P-loop fold NTPase (**Figure1A & 1B**). A distortion in the P-loop conformation makes it incompatible with the binding of nucleotides [15]. The features that contribute in preserving the architecture of this ancient motif remain unidentified and uncharacterized. Therefore, an important and open question is how P-loop forms a typical architecture in structurally and functionally diverse P-loop NTPases. Here, we used a well established closeness centrality network parameter to study the global impact of residues on the typical local conformation of P-loop. Residues with high closeness value are central in network and interact with other residues directly or by a few intermediates [8].

High closeness residue positions around P-loop and its flanking regions in Ras Super family members

In order to understand the P-loop architecture, we first analyzed the residue-residue interaction network of Ras superfamily (Ras: 5P21; Rab: 3RAB; Ran: 1IBR, Rho: 1M7B and Arf: 1R4A) experimental structures in GTP bound form. Interestingly, Walker A and its flanking regions showed high density of high closeness residue positions (**Table 1**). Here, the

high closeness centrality positions are defined as those positions with statistically significant closeness values (z-score ≥ 1.0). Five Walker A residue positions (W1, W2, W5, W6, W7), four

contiguous N-terminal residue positions (N2-N5) and two C-terminal residues (C2 and C3), flanking the Walker A, showed high closeness centrality in Ras superfamily members (**Table 1**).

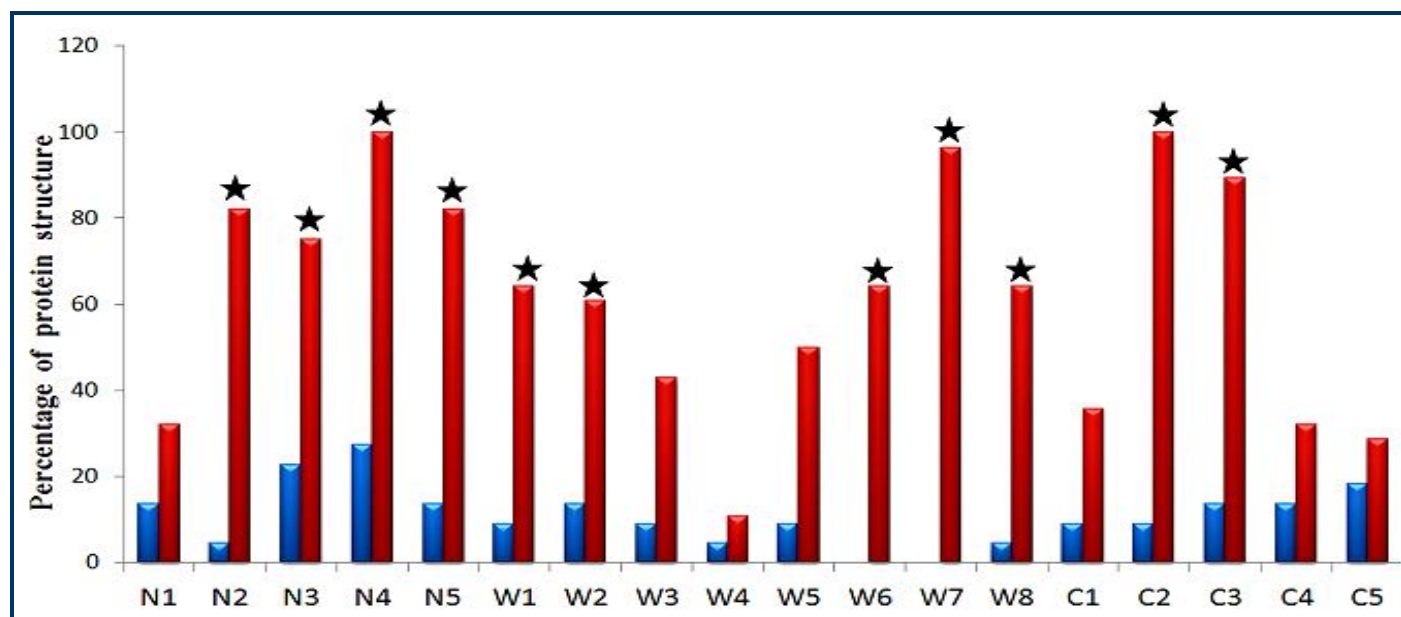


Figure 2: Bar graph showing distribution of high closeness residue positions in diverse set of P-loop NTPases (red bar). Walker A containing proteins that do not form P-loop are depicted in blue bar. High density of high closeness residue positions (star marked) shown around Walker A (W1-W8) and its flanking regions N terminal (N1-N5) and C terminal (C1-C5).

High density of high closeness residue positions in P-loop and its flanking regions in diverse set of P-loop NTPases

Since the Ras superfamily belongs to P-loop NTPase fold, we then extended the centrality analysis on high resolution X-ray crystallographic structures of P-loop NTPases (**Table 1**). The structural overlay of highly diverse P-loop NTPases fold showed that the typical P-loop architecture is maintained (**Figure 1B**). In order to avoid redundancy and utilize the diversity present in the P loop NTPases, we selected a set of 23 NTPase structures at 30% sequence identity cutoff (see **methodology**). We wanted to look at the impact of sequence diversity on the closeness value of the residues of P-loop and its flanking region. Intriguingly, the highly diverse P-loop NTPases exhibited a similar pattern of high density of conserved high closeness centrality residue positions around Walker A motif, as seen in Ras Super family. Here, the conserved high closeness centrality positions are defined as those positions with statistically significant closeness values (z-score ≥ 1.0) in at least 60% of the structures of P-loop NTPase fold (**Figure 2 & Table 1**). 11 such residue positions around Walker A and its flanking regions showed high closeness value. Four contiguous residue positions (N2-N5) of the N-terminal, two residue positions of C-terminal (C2-C3) and five residue positions of Walker A (W1, W2, W6, W7, W8) were showing high closeness centrality. The residue positions N4 (100%), W7 (96%) and C2 (100%) were highly conserved in their centrality across the diverse structures. The invariant residue positions (G, K, S/T) and variant residue positions (W2) of Walker A showed high closeness centrality (**Table 1**). Walker A sequence has wider distribution and observed in many proteins that do not bind nucleotides [7]. The structural analysis revealed that these proteins do not form the conspicuous P-loop architecture [7]. To test our prediction, we calculated the closeness value in Walker

A sequences that do not form P-loop (**Table 2**). We did not observe high density of high closeness centrality pattern.

Our results indicate the high density of conserved high closeness residue positions in P-loop and its flanking regions in P-loop fold NTPase and underscore its role in supporting the architecture of P-loop. The study presented is in concord with the observation that highly central residue positions correlate well with active site residues or their neighbors that provide supportive scaffold [13]. However, high closeness value of invariant (G, K, and S/T) residues of Walker A indicates its role in catalysis. P-loop lysine interacts and forms hydrogen-bond with oxygen of γ -phosphate of bound nucleotide and serine/threonine binds with Mg^{2+} [16, 17]. Recently Grüber *et al.* [15] demonstrated the role of conserved glycine residues of Walker A motif in guarding the active-site region for nucleotide entrance in archaea-type ATP synthases. The altered conformation of the P-loop resulted in the active-site region being closed to nucleotide entry [15].

Conclusion:

In the context of network, protein structural scaffold and sequence diversity can be visualized as a dramatic change in the type of node, and also the connections between the nodes. Regardless of such diversity, depicted in Ras superfamily and diverse domains of P-loop fold NTPase, the closeness centrality of residue positions in P-loop and its flanking regions are remarkably maintained to be high. Thus, our finding supports the observation that centrality of a residue is maintained evolutionarily to assure the proper functioning of protein [8, 13]. We did not find such high centrality residue positions in proteins containing Walker A motif that do not form P-loop. This strengthens the evidence that required geometry of

archetypal P-loop is achieved by high density of residue positions which are globally connected in short steps.

Acknowledgment:

EP acknowledges CSIR, India for the JRF and SRF. We thank Department of Bioinformatics, MMV, Banaras Hindu University, for providing computational facility.

References:

- [1] Koonin EV *et al. Trends Biochem Sci.* 2000 **25**: 223 [PMID: 10782090]
- [2] Saraste M *et al. Trends Biochem Sci.* 1990 **15**: 430 [PMID: 2126155]
- [3] Vetter IR *et al. Q Rev Biophys.* 1999 **32**: 1 [PMID: 10800520]
- [4] Walker JE *et al. EMBO J.* 1982 **1**: 945 [PMID: 6329717]
- [5] Wolf YI *et al. Genome Res.* 1999 **9**: 17 [PMID: 9927481]
- [6] Ma BG *et al. Biochem Biophys Res Commun.* 2008 **366**: 607 [PMID: 18073136]
- [7] Ramakrishnan C *et al. Protein Eng.* 2002 **15**: 783 [PMID: 12468712]
- [8] Amitai G *et al. J Mol Biol.* 2004 **344**: 1135 [PMID: 15544817]
- [9] Jacobs DJ *et al. Proteins.* 2001 **44**: 150 [PMID: 11391777]
- [10] Vendruscolo M *et al. Phys Rev E Stat Nonlin Soft Matter Phys.* 2002 **65**: 0619101 [PMID: 12188762]
- [11] Kannan N & Vishveshwara S, *J Mol Biol.* 1999 **292**: 441 [PMID: 10493887]
- [12] Thibert B *et al. BMC Bioinformatics.* 2005 **6**: 213 [PMID: 16124876]
- [13] del Sol A *et al. Protein Sci.* 2006 **15**: 2120 [PMID: 16882992]
- [14] Sobolev V *et al. Bioinformatics.* 1999 **15**: 327 [PMID: 10320401]
- [15] Kumar A *et al. J Mol Biol.* 2010 **396**: 301 [PMID: 19944110]
- [16] Crampton DJ *et al. Biochemistry.* 2001 **40**: 3710 [PMID: 11297439]
- [17] Runquist JA *et al. Biochemistry.* 2001 **40**: 14530 [PMID: 11724566]

Edited by P Kanguane

Citation: Pathak *et al.* Bioinformation 9(1): 023-028 (2013)

License statement: This is an open-access article, which permits unrestricted use, distribution, and reproduction in any medium, for non-commercial purposes, provided the original author and source are credited

Supplementary material:

Methodology:

Computation of closeness centrality

Protein structures can be represented as a residue-residue interaction graphs in which amino acid residues serve as the nodes and their interatomic contacts are the edges. Closeness centrality correlates more accurately with critical residues than any other centrality measurement tested [12]. Therefore, we used SARIG server which efficiently calculates the closeness centrality (<http://bioinfo2.weizmann.ac.il/~pietro/SARIG/V3/index.html>). Closeness centrality of node x(C(x)) is calculated as follows:

$$C(x) = (N-1) / \sum_{y \in U, y \neq x} d(x, y)$$

Where d(x, y) is the shortest-path between node x and any node y. U is the set of all nodes and N is the number of nodes in the network.

Table 1: Closeness centrality (z-scores) of residues of Walker A and flanking region sequence in P-loop NTPases H (%) is the percentage of structures with z-score ≥ 1.0 . HCR is the number of High closeness residues with z-score ≥ 1.0 .

PDB ID	N1	N2	N3	N4	N5	W1	W2	W3	W4	W5	W6	W7	W8	C1	C2	C3	C4	C5	HCR
1FMJ_A	ASP -0.147	VAL 0.819	PHE 1.025	VAL 1.712	ALA 1.696	SER 1.688	TYR 2.342	GLN 2.36	ARG 2.287	SER 1.919	GLY 1.467	THR 1.736	THR 1.413	MET 0.928	THR 1.132	GLN 0.935	GLU 0.409	LEU 0.433	12
1D2N_A	SER 0.582	VAL 1.533	LEU 1.423	LEU 1.852	GLU 1.666	GLY 1.245	PRO 1.685	PRO 1.151	HIS 0.895	SER 1.637	GLY 1.618	LYS 1.954	THR 1.704	ALA 0.968	LEU 1.637	ALA 1.647	ALA 1.378	LYS 1.387	15
1NJF_A	ALA 0.224	TYR 1.471	LEU 0.911	PHE 1.782	SER 0.774	GLY 0.665	THR 1.108	ARG 1.191	GLY 0.799	VAL 1.154	GLY 1.248	LYS 1.902	THR 2.024	SER 1.532	THR 2.058	ILE 1.771	ALA 2.426	ARG 1.708	13
1SVM_A	TYR 1.149	TRP 1.344	LEU 0.766	PHE 1.349	LYS 0.388	GLY -0.155	PRO -0.248	ILE -0.793	ASP -0.63	SER -0.169	GLY 0.548	LYS 0.938	THR 1.078	THR 1.243	LEU 1.733	ALA 1.442	ALA 1.526	ALA 2.014	9
1BIF_A	LEU 0.412	ILE 1.164	VAL 0.368	MET 1.277	VAL 0.436	GLY 0.051	LEU 0.304	PRO -0.428	ALA 0.048	ARG 0.334	GLY 1.007	LYS 1.107	THR 1.414	TYR 1.869	ILE 1.917	SER 1.193	LYS 1.976	LYS 2.772	10
1CP2_A	GLN 0.695	VAL 1.329	ALA 1.384	ILE 2.396	TYR 2.114	GLY 1.644	LYS 0.882	GLY 1.086	ILE 0.18	GLY 1.157	LYS 1.06	LYS 2.466	SER 1.615	THR 1.366	THR 2.202	THR 1.735	GLN 1.46	ASN 1.183	15
1G3Q_A	ILE 1.899	SER 1.548	ILE 2.349	VAL 1.846	SER 1.316	GLY -0.439	LYS 0.773	GLY 0.317	GLY -0.317	THR 1.186	GLY 1.082	LYS 2.468	THR 1.859	THR 1.461	THR 2.233	VAL 2.077	THR 1.244	ALA 1.232	14
1NP6_B	LEU 1.192	LEU 1.816	ALA 1.08	PHE 2.075	ALA 1.08	ALA 0.318	TRP 0.478	SER 0.212	GLY -0.42	THR 0.55	GLY 0.8	LYS 1.658	THR 1.192	THR 0.571	LEU 1.154	LEU 1.658	LYS 0.582	LYS 0.603	9
1YRB_A	ILE 1.199	VAL 1.706	VAL 1.863	PHE 2.057	VAL 2.12	GLY 1.241	THR 1.276	ALA 0.686	GLY 0.302	SER 1.089	GLY 1.863	LYS 1.039	THR 0.583	THR 1.726	THR 1.454	THR 0.322	GLY 0.656	GLU 1.2	12
2HYI_C	ASP -0.194	VAL 0.593	ILE 0.331	ALA 1.475	GLN 1.418	SER 1.412	GLN 1.469	SER 2.001	GLY 0.847	THR 1.429	GLY 1.257	LYS 2.333	THR 1.97	ALA 1.139	THR 1.192	ALA 1.807	PHE 0.902	SER 0.393	12
2J0S_A	ASP -0.218	VAL 0.567	ILE 0.301	ALA 1.468	GLN 1.317	SER 1.22	GLN 1.38	SER 2.052	GLY 0.912	THR 1.409	GLY 1.363	LYS 2.558	THR 2.052	ALA 0.876	THR 1.486	PHE 2.072	SER 1.007	ILE 0.669	12
1LY1_A	ILE 0.993	ILE 1.664	LEU 1.416	THR 2.117	THR 1.567	GLY 0.702	CYS 1.01	PRO 1.027	GLY -0.15	SER 0.64	GLY 1.01	LYS 2.16	SER 1.253	THR 0.733	TRP 1.491	ALA 1.235	ARG -0.15	GLU -0.2	11
1VHT_A	ILE 1.035	VAL 1.425	ALA 1.396	LEU 1.85	THR 1.721	GLY 1.253	GLY 0.589	ILE 0.566	GLY -0.072	SER 0.628	GLY 0.788	LYS 1.689	SER 1.115	THR 0.574	VAL 1.3	ALA 1.377	ASN 0.74	ALA 0.387	10
1H65_A	LEU 0.975	THR 1.059	ILE 1.997	LEU 1.985	VAL 1.815	GLY 1.202	LYS 1.577	GLY 0.035	GLY 0.259	VAL 0.893	GLY 0.985	LYS 1.738	SER 0.409	SER 0.717	THR 2.197	VAL 1.37	ASN 0.657	SER 0.994	9
1SVS_A	LYS -0.603	LEU 0.127	LEU 0.397	LEU 1.083	LEU 0.704	GLY 1.056	ALA 2.117	GLY 1.344	GLU 1.916	SER 1.667	GLY 1.552	LYS 1.613	SER 1.042	THR 1.499	ILE 1.691	VAL 1.315	LYS 1.159	GLN 1.002	14
2AKA_A	SER 1.363	LEU 1.46	LEU 1.735	ILE 1.808	THR 1.96	GLY 1.255	GLU 1.735	SER 1.393	GLY 0.903	ALA 1.649	GLY 1.516	LYS 1.921	THR 1.31	GLU 1.187	ASN 1.718	THR 1.436	LYS 0.717	LYS 0.855	15
2AKA_B	GLN 1.38	ILE 1.901	ALA 1.638	VAL 2.2	VAL 1.79	GLY 1.372	GLY 0.795	GLN 0.729	SER 0.154	ALA 1.074	GLY 1.248	LYS 2.053	SER 1.568	SER 1.121	VAL 2.28	LEU 2.311	GLU 1.414	ASN 1.524	15
2CXX_A	THR 0.079	ILE 0.978	ILE 1.739	PHE 2.08	ALA 1.888	GLY 1.576	ARG 1.72	SER 0.34	ASN 0.029	VAL 1.436	GLY 0.824	LYS 2.022	SER 0.104	THR 0.505	LEU 2.179	ILE 0.9	TYR 0.104	ARG 0.233	8
1GVN_B	ALA 0.569	PHE 1.189	LEU 1.222	LEU 2.165	GLY 1.495	GLY 1.495	GLN 1.785	PRO 1.957	GLY 1.469	SER 1.539	GLY 1.099	LYS 2.277	THR 0.964	SER 1.408	LEU 1.711	ARG 1.909	SER 0.894	ALA 0.848	14
1HTW_A	MET 1.342	VAL 2.316	TYR 1.837	LEU 2.462	ASN 1.264	GLY -0.295	ASP -0.424	LEU -0.347	GLY -0.866	ALA -0.106	GLY 0.459	LYS 1.264	THR 0.722	THR 0.333	LEU 1.751	THR 1.687	ARG 0.621	GLY 0.364	8
1KNQ_A	ILE 0.501	TYR 1.305	VAL 1.58	LEU 2.477	MET 2.146	GLY 1.492	MET 1.545	GLY 1.206	SER 0.286	GLY 0.846	GLY 0.772	LYS 2.288	SER 0.891	ALA 0.713	VAL 1.423	ALA 1.271	SER -0.11	GLU -0.248	10
1M7G_A	THR 1.498	ILE 2.106	TRP 2.474	LEU 2.294	THR 1.898	GLY 0.893	LEU 0.935	SER 0.425	ALA -0.477	SER 0.388	GLY 0.491	LYS 1.7	SER 0.472	THR 0.388	LEU 1.365	ALA 1.156	VAL -0.145	GLU 0.189	8
1UJ2_A	LEU 0.56	ILE 1.402	GLY 0.985	VAL 2.13	SER 1.661	GLY 0.997	GLY 1.35	THR 1.55	ALA 0.337	THR 0.739	GLY 0.75	LYS 2.146	SER 1.058	SER -0.001	VAL 1.337	CYS 1.591	ALA 0.164	LYS -0.048	9
5P21_A	LYS 0.271	LEU 1.301	VAL 1.376	VAL 2.081	VAL 1.827	GLY 1.21	ALA 0.964	GLY -0.37	VAL 0.032	GLY 0.846	LYS 1.068	LYS 1.953	SER 0.683	ALA 0.242	LEU 2.235	THR 1.192	ILE -0.116	GLN 0.51	9
3RAB_A	LYS 0.191	ILE 1.363	LEU 1.326	ILE 2.011	ILE 1.805	GLY 1.29	ASN 1.095	SER -0.248	SER -0.015	VAL 1.078	GLY 1.13	LYS 1.866	THR 1.112	SER 0.362	PHE 2.496	LEU 1.326	PHE -0.133	ARG 0.666	12
1M7B_A	LYS 0.258	ILE 1.175	VAL 1.054	VAL 1.978	VAL 1.764	GLY 1.099	ASP 1.411	SER 0.345	GLN 0.616	CYS 1.427	GLY 1.039	LYS 2.033	THR 0.603	ALA 0.511	LEU 2.28	LEU 1.331	HIS -0.169	VAL 0.577	11
1IBR_A	LYS 0.642	LEU 1.45	VAL 1.34	LEU 1.976	VAL 1.854	GLY 1.129	ASP 0.977	GLY -0.251	GLY 0.246	THR 0.977	GLY 1.216	LYS 2.059	THR 0.782	THR 0.782	PHE 2.429	VAL 1.487	LYS 0.029	ARG 0.551	9
1R4A_A	ARG 0.124	ILE 1.192	LEU 1.23	ILE 1.802	LEU 1.716	GLY 0.968	LEU 1.467	ASP -0.138	GLY -0.475	ALA 1.078	GLY 0.485	LYS 1.653	THR 0.035	THR -0.009	ILE 1.868	LEU 0.95	TYR 0.468	ARG 0.246	8
H (%)	32.14	82.14	75.00	100	82.14	64.29	60.71	42.86	10.71	50.00	64.29	96.42	64.29	35.71	100	89.29	32.14	28.57	

